Influence of climate variability, fire and phosphorus limitation on the vegetation structure and dynamics in the Amazon-Cerrado border

Emily Ane Dionizio da Silva[1], Marcos Heil Costa[1], Andrea Almeida Castanho[2], Gabrielle Ferreira Pires[1], Beatriz Schwantes Marimon[3], Ben Hur Marimon-Junior[3], Eddie Lenza[3], Fernando Martins Pimenta[1], Xiaojuan Yang[4], Atul K. Jain[5]

[1] Department of Agricultural Engineering, Federal University of Viçosa (UFV), Viçosa, MG, Brazil

[2] The Woods Hole Research Center, 149 Woods Hole Rd., Falmouth, MA USA

[3] Federal University of Mato Grosso, Nova Xavantina Campus, Nova Xavantina, MT, Brazil

[4] Oak Ridge National Laboratory, Oak Ridge, TN, USA

[5] Department of Atmospheric Sciences, University of Illinois at Urbana-Champaign

Correspondence to: Emily Ane D. da Silva (emilyy.ane@gmail.com)

Abstract

Climate, fire and soil nutritional limitation are important elements that affect the vegetation dynamics in areas of forest-savanna transition. In this paper, we use the dynamic vegetation model INLAND to evaluate the influence of inter-annual climate variability, fire and phosphorus (P) limitation on the Amazon-Cerrado transitional vegetation structure and dynamics. We assess how each environmental factor affects the net primary production, leaf area index and aboveground biomass (AGB), and compare the AGB simulations to observed AGB map. We used two regional datasets − the 1961-1990 average seasonal climate and the 1948 to 2008 inter-annual climate variability, two datasets of total soil P content in soil, based on regional (field measurements) and global data and the INLAND fire module. Our results show that inter-annual climate variability, P limitation and fire occurrence gradually improve simulated vegetation types and these effects are not homogeneous along the latitudinal/longitudinal gradient, showing a synergistic effect among them. In terms of magnitude, the effect of fire is stronger, and is the main driver of vegetation changes along the transition. The nutritional limitation, in turn, is stronger than the effect of inter-annual climate variability acting on the transitional ecosystems dynamics. Overall, INLAND typically simulates more than 80% of the AGB variability in the transition zone. However, the AGB in many places is clearly not well simulated, indicating that important soil and physiological factors in the Amazon-Cerrado border, such as lithology and water table depth, carbon allocation strategies and mortality rates, still need to be included in the model.

1 Introduction

The Amazon and Cerrado are the two largest and most important phytogeographical domains in South America. The Amazon forest has been globally recognized and distinguished not only for its exuberance in diversity and species richness, but also for playing an important role in the global climate by regulating water (Bonan, 2008; Pires and Costa, 2013) and heat fluxes (Shukla et al., 1990; Rocha et al., 2004; Roy et al., 2002). The Cerrado is recognized worldwide for being the richest savanna in the world (Myers et al., 2000; Klink and Machado, 2005). It is characterized by different physiognomies, ranging from sparse physiognomies to dense woodland formations, and the latter are commonly mixed with Amazon rainforest forming transitional areas. The Amazon-Cerrado transition extends for 6270 km from northeast to southwest in Brazil, and the ecotonal vegetation around this transition is a mix of the characteristics of the tropical forest and the savanna (Torello-Raventos et al., 2013).

Gradients of seasonal rainfall and water deficit, fire occurrence, herbivory and low fertility of the soil have been reported as the main factors that characterize the transition between forest and savanna globally (Lehmann et al., 2011; Hoffman et al., 2012; Murphy and Bowman, 2012). However, few studies have evaluated the individual and combined effects of these factors on Brazilian ecosystems ecotones (Marimon-Junior and Haridasan, 2005; Elias et al., 2013; Vourtilis et al., 2013).

It is challenging to assess the degree of interaction among these various environmental factors in the transitional region and to infer how each one influences the distribution of the regional vegetation. In this case, Dynamic Global Vegetation Models (DGVMs) can be powerful tools to isolate the influences of climate, fire and nutrients, therefore helping to understand their large-scale effects on vegetation (House et al., 2003; Favier et al., 2004; Hirota et al., 2010; Hoffman et al., 2012).

Previous modelling studies using DGVMs that investigate climate effects in the Amazon indicate that the rainforest could experience changes in rainfall patterns which would either transform the forest into an ecosystem with more sparse vegetation – similar to a savanna, what has been called as the "savannization of the Amazon" (Shukla et al., 1990; Cox et al., 2000; Oyama and Nobre, 2003; Betts et al., 2004; Cox et al., 2004; Salazar et al., 2007) - or to a seasonal forest (Malhi et al., 2009; Pereira et al., 2012; Pires and Costa, 2013). These studies had great importance to the improvement of terrestrial biosphere modeling, but they neglect two important processes in tropical ecosystem dynamics: fire occurrence and nutrient limitation, particularly the Phosphorus (P) limitation.

In tropical ecosystems, fire plays an important ecological role and influences the productivity, the biogeochemical cycles and the dynamics in the transitional biomes, not only by changing the phenology and physiology of plants, but also by modifying the competition among trees and lower canopy plants such as grasses, shrubs and lianas. Fire occurrence, depending on its frequency and intensity, may increase the mortality of trees and transform an undisturbed forest into a disturbed and flammable one (House et al., 2003; Hirota et al., 2010; Hoffmann et al., 2012). Fires also affect the dynamics of nutrients in the savanna ecosystem, changing mainly the N:P relationship and P availability in the soil (Nardoto et al. 2006).

Studies suggest that P is the main limiting nutrient within tropical forests (Malhi et al., 2009; Mercado et al., 2011; Quesada et al., 2012) unlike the temperate forests. Phosphorus is a nutrient that is easily adsorvided by soil minerals due to the large amount of iron and aluminum oxides in the Amazon and Cerrado acidic and strongly weathered soils (Dajoz, 2005; Goedert, 1986). In the tropics, the warm and wet climate favors the high biological activity in the soil and the litter decomposition, not limiting

78 the nitrogen for plant fixation. In Cerrado, higher soil fertility is related to regions with greater woody
79 plants abundance and less grass cover, similarly to the features found in the Amazon rainforest (Moreno
80 et al., 2008; Vourtilis et al., 2013; Veenendaal et al., 2015). However, the phosphorus limitation is often
81 neglected by DGVMs. which usually assume unlimited P availability and consider nitrogen as the main
82 limiting nutrient. However, N is not a limiting nutrient for trees in the tropics (Davidson et al. 2004),
83 while P availability affects the trees dynamics.

84 In principle, in transitional forests, where the climate is intermediate between wet and seasonally
85 dry, the heterogeneous structure and phenology make it difficult to represent these forests in models.
86 The Amazon-Cerrado border is the result of the expansion and contraction of the Cerrado into the forest
87 (see Marimon et al., 2006; Morandi et al., 2016), especially in the Mato Grosso state, where extreme
88 events, such as intense droughts, influence the vegetation dynamics (Marimon et al., 2014) and the
89 nutrient (Oliveira et al., 2017) and carbon cycling (Valadão et al., 2016).

90 Currently, no model has demonstrated to be able to accurately simulate the vegetation transition
91 between Amazonia and Cerrado. In general the DGVMs simulate evergreen forest along the Amazon-
92 Cerrado border and neglect savanna occurrence (Botta and Foley, 2002; Bond et al., 2005; Salazar et al.,
93 2007; Smith et al., 2014). This difficulty may be due to absence or not well represented disturbances
94 such as fire, nutritional limitation or soil proprieties. Thus, we need a better understanding of the drivers
95 on transitional vegetation to determine the parameters and establish relations between the environmental
96 and transitional vegetation physiognomies.

97 In this paper we use the dynamic vegetation model INLAND (Integrated Model of Land Surface
98 Processes) to evaluate the influence of inter-annual climate variability, fire occurrence and P limitation

in the Amazon-Cerrado transitional vegetation dynamics and structure. We assess how each element affects the net primary production (NPP), leaf area index (LAI) and aboveground biomass (AGB) and compare the model simulated AGB to observed AGB data. The results presented here are important to build models that accurately represent the transition vegetation, and show the need to include the spatial variability of eco-physiological parameters in these areas.

2 Materials and methods

2.1 Study Area

The present study focuses on the Amazon-Cerrado transition (Figure 1). We use the official delimitation of the Brazilian biomes proposed by IBGE (2004), and define five transects along the transition border with 1° × 1° grid size (the terms "transition", "Amazon-Cerrado transition" and "Forest-Savanna transition" are used interchangeably with the same meaning throughout this manuscript).Transects 1 to 4 are established considering approximately 330 km into the Amazon and 330 km into the Cerrado domain, while Transect 5 is 880 km long on the southern Amazon-Cerrado border. The transects are located as follows: Transect 1 (T1, 44°- 50°W; 5°- 7°S), Transect 2 (T2, 46°-51° W; 7°-9S), Transect 3 (T3, 48°-54° W; 9°-11° S), Transect 4 (T4, 49° - 55° W; 11°-13° S), and Transect 5 (T5, 52° - 60° W; 13°-15° S) (Figure 1).

2.2 Description of the INLAND Surface Model

The Integrated Model of Land Surface Processes (INLAND) is the land-surface component of the Brazilian Earth System Model (BESM). INLAND is basically a revision of the IBIS model (Integrated Biosphere Simulator, described by Foley et al., 1996; Kucharik et al., 2000), through

assembly and standardization of different IBIS versions, and improvements in software engineering. We used the version described by Senna et al. (2009) as starting point for INLAND. No changes in tuning were done since that paper, except the addition of the P parameterization, described below.

The model considers changes in the composition and structure of vegetation in response to the environment and incorporates important aspects of biosphere-atmosphere interactions. The model simulates the exchanges of energy, water, carbon and momentum between soil-vegetation-atmosphere. These processes are organized in a hierarchical framework and operate at different time steps, ranging from 60 minutes to 1 year, coupling ecological, biophysical and physiological processes. The vegetation structure is represented by two layers: upper (arboreal PFTs) and lower (no arboreal PFTs, shrubs and grasses) canopies, and the composition is represented by 12 plant functional types (PFTs) (e.g., tropical broadleaf evergreen trees or C4 grasses, among several others).The photosynthesis and respiration processes are simulated in a mechanistic manner using the Ball-Berry-Farquhar model (details in Foley et al., 1996). The vegetation phenology module simulates the processes such as budding and senescence based on drought phenology scheme for tropical deciduous trees. The dynamic vegetation module computes the following variables yearly for each PFT: gross and net primary productivity (GPP and NPP), changes in AGB pools, simple mortality disturbance processes and resultant LAI, thus allowing vegetation type and cover to change with time. The partitioning of the NPP for each PFT resolves carbon in three AGB pools: leaves, stems and fine roots. The LAI of each PFT is obtained by simply dividing leaf carbon by specific leaf area, which in INLAND is considered fixed (one value) for each PFT.

139 INLAND has eight soil layers to simulate the diurnal and seasonal variations of heat and
140 moisture. Each layer is described in terms of soil temperature, volumetric water content and ice content
141 (Foley et al., 1996; Thompson and Pollard, 1995). Furthermore, all of these processes are influenced by
142 soil texture and amount of organic matter within the soil profile.

143 Considering these aspects of vegetation dynamics and soil physical properties the model can
144 simulate plant competition for light and water between trees, shrubs and grasses through shading and
145 differences in water uptake (Foley et al., 1996). These PFTs can coexist within a grid cell and their
146 annual LAI values indicate the dominant vegetation type within a grid cell. For example, the dominant
147 vegetation type is a Tropical Evergreen Forest if the PFT tropical broadleaf evergreen tree has an annual
148 mean upper canopy LAI (LAI_{upper}) above 2.5 m^2 m^{-2}. On the other hand, the dominant vegetation type is
149 a Tropical Deciduous Forest if the tropical broadleaf drought-deciduous tree has an annual mean
150 LAI_{upper} above 2.5 m^2 m^{-2}. Where total tree LAI (LAI_{upper}) is between 0.8 and 2.5 m^2 m^{-2}, dominant
151 vegetation type is savanna, and LAI_{upper} values smaller than 0.8 m^2 m^{-2} characterize a grassland
152 vegetation type.

153 We assume that the vegetation types Tropical Evergreen Forest and the Tropical Deciduous
154 Forest in INLAND represents the Amazon rainforest, while Savanna and Grasslands represent the
155 Cerrado. Savanna would be equivalent to the Cerrado physiognomies *Cerradão* and *Cerrado sensu*
156 *strictu*, while Grasslands would be equivalent to the physiognomies *Campo sujo* and *Campo Limpo*
157 (*sensu* Ribeiro and Walter, 2008).

158 The soil chemical properties are represented by the carbon, nitrogen and phosphorus. The carbon
159 cycle is simulated through vegetation, litter and soil organic matter, where the biogeochemical module

is similar to the CENTURY model (Parton et al., 1993; Verberne et al., 1990). The amount of C existing in the first meter of soil is divided into different compartments characterized by their residence time, which can vary in an interval of hours for microbial AGB and organic matter to several years for lignin. The model considers only the soil N transformations and carbon decomposition, but the N cycle is not fully simulated and N does not influence the vegetation productivity, i.e., there is a fixed C:N ratio. The P cycle also is not fully implemented, instead the P-limitation is spatially parameterized through the linear relation developed by Castanho et al. (2013) to limit the gross primary productivity. A map of total P available in the soil (P_{total}) is used by the model to estimate the maximum capacity of carboxylation by the Rubisco enzyme (V_{max}) for each grid using Equation (1) :

$$V_{max} = 0.1013\, P_{total} + 30.037 \qquad (1)$$

where V_{max} and P_{total} are given in $\mu molCO_2\ m^{-2}\ s^{-1}$ and $mg\ kg^{-1}$, respectively. This equation has been based on data for tropical evergreen and deciduous trees, and is applied only to these two PFTs, while the other PFTs are unaffected.

INLAND also contains a spatial fire module, from the Canadian Terrestrial Ecosystem Model CTEM (Arora and Boer, 2005). In this module, three aspects of the fire triangle are considered – the availability of fuel to burn, the flammability of vegetation, and the presence of an ignition source. Each is represented daily by an independently calculated probability and the product of the three is the probability of fire occurrence. Availability of fuel to burn depends on biomass, flammability depends on soil moisture and ignition depends on a random lightning occurrence and a constant anthropogenic ignition probability (in these runs prescribed to 0.50). The burned area fraction is calculated daily and depends on the probability of ignition, spread rate (as function of wind speed, soil moisture), simulated

length to breadth ratio of fire, and extinguishing rate. The daily area burned is accumulated through the year and its ratio to the grid cell area is applied at the end of each year as a "penalization fraction" to leaf, wood and root biomass pools. For more details, see Arora and Boer (2005).

2.3 Observed data

2.3.1 Phosphorus databases

We used two P databases to estimate V_{max} (Equation 1): one regional (referred to as PR) and one global database (referred to as PG). In addition, a control P map (PC) represents the unlimited nutrient availability case, equivalent to a V_{max} of 65 $\mu molCO_2\ m^{-2}\ s^{-1}$, or 350 mg P kg^{-1} soil, according to Equation 1.

The PR database was developed from total P in the soil for the Amazon basin published by Quesada et al. (2011) plus 54 additional available P samples (P extracted via Mehlich-1 extractor, $P_{mehlich\text{-}1}$) (Figure 2a). We used the $P_{mehlich\text{-}1}$ and clay contents measured in a forest-savanna transition region in Brazil (Mato Grosso state) to estimate P_{total} and expand the coverage area of the P data (Section S1). These 54 samples were gridded to a 1° × 1° grid to be compatible with the spatial resolution used by INLAND, resulting in 12 additional pixels with observed total P content (Figure 2a). For pixels without observed P_{total}, the P_{total} was assumed to be 350 mg P kg^{-1} soil, similarly to the PC conditions.

A global dataset of P_{total} (Figure 2b) was also used to estimate V_{max}. This global data set is part of a database containing six global maps of the different forms of P in the soil (Yang et al., 2013). The P_{total} was estimated from lithologic maps, distribution of soil development stages, fraction of the

201 remaining source material for different stages of weathering using chronosequence studies (29 studies),
202 and P distribution in different forms for each soil type based on the analysis of Hedley fractionation
203 (Yang and Post, 2011), which are part of a worldwide collection of soil profile data. The uncertainties
204 and limitations associated with this database are restricted to the Hedley fractionation data used, which
205 are 17% for low weathered soils, 65% for intermediate soils and 68% for highly weathered soils (Yang
206 et al., 2013).

207 **2.3.2 Above-Ground Biomass (AGB) database**

208 The AGB database used was created by Nogueira et al. (2015) and considered undisturbed (pre-
209 deforestation) vegetation existing in the Brazilian Amazonia. This database was compiled from a
210 vegetation map at a scale of 1:250000 (IBGE, 1992) and AGB averages from 41 published studies that
211 had conducted direct sampling in either forest (2317 plots) or non-forest or contact zones (1830 plots).
212 We bi-linearly interpolated the AGB (dry weight) for each transect considering 1° × 1° to ensure
213 compatibility of the observed and simulated data.

214 Five longitudinal transects (Figure 1) were used separately to characterize AGB in the Amazon-
215 Cerrado border (Figures 3a and 3b). In T1, T2, T3 and T4, the higher AGB values in the west and lower
216 values in the east are consistent with the transition from a dense and woody vegetation (the Amazon
217 forest) towards a sparse vegetation with lower AGB (the Cerrado). However, T1 shows a more gradual
218 reduction of AGB along the west to east gradient, while in T2, T3 and T4 the transition is more abrupt.
219 In T5 no west-east gradient is present with high AGB heterogeneity and predominant low AGB across
220 the transect (Figure 3b).

221

2.4 Simulations

The model was forced with the prescribed climate data based on the Climate Research Unit (CRU) database (Harris et al., 2014). Two climate boundary conditions were used: the first is referred to as the monthly climatological average (CA) that represents the average climate for the period 1961-1990. The second climate boundary condition is the historical dataset, for the continuous period between 1948 and 2008 (CV). For both boundary conditions, the variables used are rainfall, solar radiation, wind velocity and maximum and minimum temperatures. The CRU database has been widely used by the scientific community in case studies, because these data preserve the spatial mean of the rainfall data, although, they do not provide adequate representation of their variance precipitation (Beguería et al., 2016). The dataset has a 1-degree spatial resolution and a monthly time resolution.

Soil texture data is based on the IGBP-DIS global soil (Global Soil Data Task 2000) (Hansen and Reed, 2000). In the CV group of runs, the model was spin-up by cycling the 1948-2008 climate data (61-year) seven times, totaling 427 years. In the CA group of runs, the annual mean climate data was cycled 427 times. In both cases, CO_2 varied from 278 to 380 ppmv, according to observations in the period, updated annually. In both cases, only the model results of the last 10 years were used to analyze the results.

The experiment design is a factorial combination of the climate scenarios (CA, monthly climatological average, 1961-1990; CV, monthly climate time series, 1948-2008), the nutrient limitation on V_{max} (PC, no P limitation (V_{max} = 65 $\mu molCO_2\, m^{-2}\, s^{-1}$); PR, regional P limitation; PG, global P limitation) and the occurrence of fire (F) or not (Table 1). The 12 combinations in Table 1 allow the evaluation of individual and combined effects of climate, soil chemistry, and the incidence of fire on the

variables: Net Primary Production (NPP), tree AGB, and LAI of the upper and lower canopies (LAI_{upper}, LAI_{lower}).

We consider that the subtraction between the simulations (CV+PC) and (CA+PC) represents the isolated effect of inter-annual climate variability without P limitations. The same logic is applied to isolate other factors such as fire and P in different climate scenarios. For example, the fire effect under average climate without P limitation case is calculated by the difference between CA+PC+F and CA+PC. Similarly, the isolated effect of fire under a climate with inter-annual variability scenario without influence of P limitation is calculated by the difference between CV+PC+F and CV+PC. The different combinations of climate scenarios with and without fire effects and with and without P limitations are described in Table 2.

2.5 Statistical analysis and determination of the best model configuration

The statistical analysis is divided in four parts. First, we present maps of the isolated effects for all simulated area calculated as the average of the last ten years of simulated spatial patterns. The statistical significance of the isolated effects on NPP, LAI and AGB are determined using the t-test with $p < 0.05$. The results are tested in each pixel, for all the simulated domain ($n = 10$).

Second, we present an analysis of variance using the one-way ANOVA and the Tukey-Kramer test in the transition zone. We consider all 31 pixels which fall in transects T1 to T5 (n_{pixels}). The results presented are based on the set of last 10 years of simulation (1999-2008, n_{years}) for the 12 combinations ($n_{simulation}$) in Table 1. Moreover, we grouped treatments according to climate regardless of P limitation, presence or absence of fire, where all sets with CV vs CA are tested (Group 1, n=1860, (n_{pixel} x n_{year} x ($n_{simulation}$/2)). Similarly, in Group 2 we tested if PC, PR or PG were significantly different from each

other regardless the F or climate used (Group 2, n=1240, (n_{pixel} x n_{year} x ($n_{simulation}$/3)). In Group 3 we tested if fire introduced a significant effect regardless of climate and P limitation (Group 3, n=1860, (n_{pixel} x n_{year} x ($n_{simulation}$/2)). Finally, all treatments were tested to each simulation assessing their individual effects on NPP, LAI and AGB (n_{pixel} x n_{year} = 310).

Third, a correlation coefficient between the simulated and observed values for AGB was calculated for each transect. The simulated variables are averaged for the last 10 years of simulations (1999 - 2008) and compared to AGB from Nogueira et al. (2015) within a grid cell.

Finally, we evaluate INLAND's ability to assign the dominant vegetation type by analyzing 10 years of probability of occurrence. If the dominant vegetation type (evergreen tropical forest, or deciduous forest for the Amazon rainforest, and savanna or grasslands for Cerrado) in a pixel is the same in more than 90% of the simulated years (9 out of 10), then the simulated vegetation type is defined as "very robust" for that pixel; if it occurs in 70 - 90% of the simulated years, the simulated result is considered to be "robust". If the dominant vegetation occurred in less than 70% of simulated years, the pixel is considered "transitional" vegetation.

3 Results

3.1 Influence of climate, fire and phosphorus in the Amazon-Cerrado transition region

3.1.1 Spatial patterns

Overall, the inclusion of inter-annual climate variability (CV) resulted in a decrease in the simulated average tree biomass (TB) by 3.8% in the entire Brazilian Amazonia, and by 8.7% in the entire Cerrado in comparison to average climate (CA), with values obtained by the difference CV+PC –

284 CA+PC (Figure 4a). The spatial differences between CV and CA for TB simulations are statistically
285 significant and range from -3 kg-C m^{-2} to +2 kg-C m^{-2}. The state of Pará, with higher influence of the El
286 Niño phenomenon, experienced the highest decrease in TB in the CV simulation. In the state of
287 Roraima, on the other hand, there was an increase of about 2 kg-C m^{-2} in TB when CV was considered.
288 Bolivia and southwest of Mato Grosso state also presented, in some grids points, a significant increase
289 in AGB higher than 2 kg-C m^{-2}.

290 On average, P acts as a limiting factor in the simulated TB, decreasing by 13% in regional P
291 (PR) simulation and 15% in global P (PG) simulation. In PR, TB decreased mainly in the southeastern
292 Amazonia (between Pará and northeastern Mato Grosso states) and northwestern Amazonas state
293 (Figure 4b). In PG, the largest TB decline occurred in central Amazonia, northeastern Pará and
294 northeastern Mato Grosso (Figure 4c). In Cerrado, on the other hand, TB declined by 2% for PR and 9%
295 for PG with respect to the control simulation. In PR, the few pixels in the Cerrado that have P limitation
296 showed a significant decrease in TB (Figure 4b), while in PG the TB reduction was statistically
297 significant for most of the Cerrado domain, except in southern Tocantins state (Figure 4c).

298 The tree biomass reduction due to fire events is much higher in magnitude than due to P
299 limitation or inter-annual climate variability (Figure 4d). The small or null fire effect in the Central
300 Amazon rainforest is related to the greater water availability in Amazonia, which makes the forest
301 naturally not flammable as well as a gradient towards seasonally dryer climate increases the intensity
302 and magnitude of fire effects towards the Cerrado (Figure 4d). The fire effect on TB over the Amazon
303 domain was 21-24% of the P limitation effect (range for PR and PG cases), while the fire effect on TB

304 over the Cerrado was more than 250% of the P limitation effects in CV simulations, which is due to
305 quick growth of grasses after fire occurrence in the latter.

306 **3.1.2 Influence of climate, fire and phosphorus in the transects**

307 Results of the ANOVAs and Tukey-Kramer test indicate that the inclusion of CV, limitation by
308 P (PR and PG) and fire in INLAND led to significantly different averages of NPP, LAI and AGB in the
309 transition zones. This influences of climate, P and fire are shown separately in Tables 3 to Table 5 and
310 combined in Table 6.

311 The effects of climate and P on productivity show that CV reduces the NPP from
312 0.68 kg-C m^{-2} yr^{-1} to 0.64 kg-C m^{-2} yr^{-1} (Table 3) and the P effect results in NPP decline from
313 0.71 kg-C m^{-2} yr^{-1} to 0.64 kg-C m^{-2} yr^{-1} (both PR and PG) (Table 4). The fire effect, moreover, has a
314 positive effect on NPP from 0.66 kg-C m^{-2} yr^{-1} when fire is off to 0.67 kg-C m^{-2} yr^{-1} when fire is on.
315 This difference, albeit low, is statistically significant (Table 5).

316 In addition CV and P limitation reduce the LAI_{total} in the canopy (Table 3 and Table 4),
317 increasing three times LAI_{lower} and decreasing LAI_{upper} (Table 5). The magnitude of fire effect on AGB
318 (46.7%, Table 5) is greater in relation to the CV (5%, Table 3) and P (14%, Table 4) limitation effects.

319 Even though CV effects on NPP and AGB for each simulation is not statistically significant, the
320 effects of fire and P limitation (regardless of phosphorus map) are. Fire effects are significant only for
321 structural variables as AGB, LAI_{total}, LAI_{upper} and LAI_{lower}. It presents an increase of LAI total of
322 1.52 m^2 m^{-2} in CV+PG+F in relation to CV+PG, and of 1.32 m^2 m^{-2} in CV+PR+F in relation to CV+PR
323 (Table 6).

3.1.3 West-East patterns of AGB in the Amazon-Cerrado transition

The model used in this study simulates > 80% of the observed AGB variability in all treatments along the transition area except in T5 (Table 7). It shows that the model is able to capture AGB variability along the transition area, which is relevant when compared to studies that simulate 50% of the observed AGB variability (Senna et al., 2009; Castanho et al., 2013).

It is not possible to identify a treatment that best represents AGB in all transects (Table 7). A combined analysis of Table 7 and Figure 5 indicates a general agreement that observed AGB decreases from W to E in T1 to T4, and this is well captured by several configurations of the model, with specific differences among them. Overall, CA and PC configurations, being the least disturbed treatments, yield higher AGB, while the introduction of CV, PG and F reduce the AGB. However, the simulated results may be above or below the observed ones, which suggests that additional local factors are not included in the model.

The curves of AGB (Figure 5) show the impact of CV, PG and F along the W-E transition. PG has a high influence on the transition, decreasing the ABG especially in the western part of the transects, where the Amazon vegetation is predominant. This feature is particularly simulated in T3 and T4, where PG decrease the AGB by 2 kg-C m^{-2} in the west pixels of these transects (Figure 5). In T1, T2 and T5, AGB decline is also higher with P limitation when compared to the curves limited only by CV. However, in T1 model simulations tend to underestimate the highest and the lowest AGB extremes, and the absolute values were always underestimated, despite the improvement in correlation with the inclusion of the fire component (Table 7).

In T2, T3 and T4, however, fire is responsible for altering the simulated AGB to the observed AGB in the eastern pixels of the Cerrado domain (Figure 5). In T5 these relations are similar, with climate presenting less influence on AGB decrease than P, and fire appears mainly as an AGB reduction factor.

3.2 Simulated composition of vegetation

Most of the pixels in CA show very robust simulations, with more than 90% of the same vegetation cover in the simulated last 10 years (Figure 6a-c and 6g-i). A larger number of pixels with transitional vegetation were simulated in CV (Figure 6d-f and and 6j-l). An even higher variability in CV compared to CA simulations was observed when we added the effects of P limitation and fire (Figure 6a and 6j-l).

The vegetation composition in all P limitation scenarios for CA simulations resulted in robust simulations for nearly all pixels, except for the north of Cerrado domain (Figures 6a, 6b and 6c). The CA+PC and CA+PR simulations had the same vegetation composition, while CA+PG replaced the deciduous forest by evergreen forest in the central Cerrado region, around 8°S 46°W (Figures 6A, 6B and 6C). This behavior might be related to the higher P_{total} values in PG than PR and PC for the Cerrado region (Figure S1). Cerrado was better represented in CV+PC, CV+PR and CV+PG than in the same CA combinations (Figure 6). The occurrence of forested areas in central Cerrado decreased in CV combinations, these being replaced by the savanna or grassland vegetation class.

When the effect of fire was added to CA simulations, the model simulated an increase in the uncertainty on the vegetation cover classification in the Cerrado region. The effect of fire reduced the presence of deciduous forest in central Cerrado biome as well as in CA+PC, and the vegetation was

365 replaced by evergreen forest in about 5 pixels with clay soils with large water retention capacity in
366 CA+PC+F (Figures 6G, 6H, 6I). In this situation, where there is little water stress in the CA simulation,
367 both evergreen and drought deciduous PFTs have each one very high LAI, and the PFT that dominates
368 can be defined by minor effects. Fire, although active, is probably too small to be relevant in a non-
369 stressed ecosystem. In CV simulations, however, fire effect results in the replacement of the deciduous
370 and perennial forest by savanna and grasses in all central Cerrado region (Figures 6J, 6K and 6L). These
371 results show the limitations of CA and the importance to consider the interannual climate variability on
372 simulations to improve the vegetation simulated.

373 For all combinations used, transitional forest areas in the northern and southwestern Cerrado
374 biome are not adequately represented. With >90% of concordance, INLAND assigns the existence of
375 tropical evergreen forest rather than deciduous forest in some pixels in the north of the transition, and
376 the existence of tropical evergreen forest rather than savanna in the southwest, indicating difficulty to
377 simulate transitional vegetation in these regions.

378 **4 Discussion**

379 The inclusion of CV, PR and PG and fire in INLAND showed significant influences on the
380 simulated vegetation structure and dynamics in the Amazon-Cerrado border (Figure 4 and Table 6),
381 suggesting that these factors play key role on vegetation structure in the forest-savanna border and can
382 improve the simulated representation of the current contact zone between these biomes. This is broadly
383 consistent with the literature that investigated causes of savanna existence in the real world (Hoffmann
384 et al., 2012; Dantas et al., 2013; Lehmann et al., 2014). In this study, the spatial analysis and the Tukey-
385 Kramer test (TK) show a difference in magnitude among these factors in vegetation, with fire

386 occurrence and P limitation being stronger than inter-annual climate variability along the transects
387 (Figure 4).

388 The spatial analysis showed that CV declines AGB predominantly in eastern Amazonia (Figure
389 4a). Climate of this region is intensely affected by El Niño–Southern Oscillation (ENSO), which could
390 reduce precipitation by 50%, placing the vegetation under intense water stress (Botta and Foley, 2002;
391 Foley et al. 2002; Marengo et al., 2004; Andreoli et al., 2012; Hilker et al., 2014). This reduction in
392 rainfall in dry years brings in direct changes in carbon flux (NPP) and stocks in leaves and wood,
393 leading to changes in vegetation structure. In addition to inter-annual changes in the rainfall, inter-
394 annual variability in other climate variables in CV also affect AGB, as average, maximum and
395 minimum temperature, as well as wind speed and specific humidity, and influence photosynthesis on
396 the model both directly (through Collatz and Farquhar equations) and indirectly (e.g. through
397 evapotranspiration). Our results showed significant differences for most part of the biomes, except
398 central Amazonia (Figure 4a), where CV and precipitation seasonality have been pointed as secondary
399 effects on vegetation (Restrepo-Coupe et al., 2013), since there is no shortage of water availability
400 during the dry season.

401 Along the Cerrado, lower water availability in some years in CV affects tree biomass, although
402 that vegetation is predominantly grassy-herbaceous. The AGB decline is significant for most part of the
403 simulated Cerrado domain (Figure 4a) and average values could represent half the amount of typical
404 tree biomass in this biome. This reduction in AGB reflects INLAND's ability to simulate similar
405 Cerrado conditions and expose the few trees to high water stress.

406 Throughout the transects, however, no significant difference was found for average AGB
407 between CV+PC and CA+PC by TK at $p<0.05$ (Table 6). On the other hand, when we analyzed the
408 influence of CV for the same pixels, but using all simulations (Table 3), regardless of P limitation and
409 fire occurrences, the results showed that the decrease in AGB by 0.38 kg-C m^{-2} (5.7%) is statistically
410 significant along the transition.

411 P limitation effect was statistically significant for PR and PG along all the Amazon domain and
412 the main differences between these simulations were the spatial patterns of tree AGB decrease (Figure
413 4b and Figure 4c). We cannot affirm which of these databases is better because they are the results of
414 different methodologies and observations (Quesada et al., 2009; Yang et al., 2014). However, PG
415 showed a higher AGB decrease in central Amazonia, northeastern Pará and northeastern Mato Grosso
416 state, indicating that in these areas the P limitation is higher. This result does not corroborate the
417 northwest-southeast AGB gradient found in the Amazon basin, which showed a higher productivity in
418 the west where soils are more fertile than those found in the southeast (Aragão et al., 2009; Saatchi et
419 al., 2007; Nunes et al., 2012; Lee et al., 2013). On the other hand, PR AGB agrees with the northwest-
420 southeast gradient, presenting less limitation in the soils of central Amazonia with declines in AGB
421 mainly in the southeastern part of the rainforest (between Pará and northeastern Mato Grosso states)
422 (Figure 4b).

423 In Cerrado, P limitation also influenced vegetation (Figure 4c) and presented statistically
424 significant differences when compared CV+PG – CV+PC. In this biome, as well as in the Amazon, tree
425 abundance richness and diversity have been generally associated with increases of soil fertility (Long et

al., 2012; Vourtilis et al., 2013), highlighting the importance of P in the composition and maintenance of vegetation, especially in transition areas.

Compared to the Amazon domain, the magnitude of effects of P limitation is lower in the Cerrado. However, few pixels in PR that have P limitation showed a significant decrease in arboreal AGB (Figure 4b), while in PG, we found reduction of AGB for most of the Cerrado domain, except only for the southern Tocantins state (Figure 4c). Despite the differences in spatial patterns, there was no statistically significant differences between PR and PG within the transects (Table 4 and Table 6).

The spatial difference between PG and PR showed that PG is lower than PR in the western Amazonia, and higher in northern Amazonia. Moreover, PG have low P values in south of the transition compared to PR, while in Cerrado domain P values ranged between 120 to 200 mg kg^{-1} (Figure S1). Although the PR dataset includes every known P data collected in the region, these differences reinforce the need to improve the data of P_{total} in the soils of the Amazon and Cerrado/Amazon transition domains. Currently, P_{total} data in Cerrado is scarce, and make unfeasible to establish a proxy similar to Castanho et al. (2013), which was specific for the Amazon.

In INLAND, the simple P-limitation parameterized through the linear relation Vmax and P_{total}, showed significant spatially differences in AGB simulated and an improvement in simulations, highlighting the importance of P-limitation in modeling studies. For the most part, Dynamic Global Vegetation Models (DGVMs) do not consider the complete phosphorus cycle (see exceptions in Goll et al., 2012 and Yang et al., 2014), despite the importance of nutrient cycling for AGB maintenance and tropical vegetation dynamics in dystrophic soils. For example, nutrient cycling in the Amazon/Cerrado transition is closely related to the hyper-dynamic turnover of the AGB (Valadão et al. 2016), in which

447 some key species might also be crucial to the hyper-cycling of nutrients through which vegetation
448 sustain the constant input of nutrients, including large annual amounts of available P (Oliveira et al.
449 2017).

450 The fire occurrence is an important factor controlling the AGB dynamics in the Cerrado or in the
451 transition vegetation (Hoffman et al.,2003; Hoffman et al., 2012; Silvério et al., 2013; Couto-Santos et
452 al., 2014; Balch et al., 2015), which this study clearly replicates, showing statistically significant
453 influences when compared to control simulations (Figure 4d and Table 5). In the transition, the fire
454 effect may reduce average AGB by 50% (Table 5), which under climate change or deforestation
455 conditions may lead to an even stronger change in the vegetation structure and dynamic. According to
456 Hoffmann et al. (2009) the undisturbed forests in the Amazon-Cerrado border appear to be more
457 resilient to fire in relation to the other tropical forests and the vegetation-fire dynamics is mainly
458 controlled by tree "topkill" (defined by the authors as complete death of the aerial biomass). In
459 INLAND, the effect of fire on AGB is similar to the "topkill" presented by Hoffmann et al. (2009),
460 being represented by the penalization fraction described earlier, and applied annually to the leaf, wood
461 and root biomass pools of the pixel. Therefore, at the end of every year both upper and lower LAI are
462 decreased, according to the amount burned, triggering competition between both canopies for light, and
463 increasing the photosynthesis rates and stocks of carbon in leaves, stems and roots pools in the lower
464 canopy. The carbon allocation in INLAND is fixed and is not modified after fire occurrence, as
465 observed in some species of the savanna-forest transition (Hoffman et al., 2009; 2012). Thus, during
466 recovery from a fire, the vegetation dynamics follows the model standard procedure.

467 In the Cerrado domain, the simulated fire effect implies in significant increases in shrubs and
468 herbaceous vegetation and decreases in the arboreal component, resulting in increment of LAI_{lower} and
469 decrease of LAI_{upper} (Table 5). These changes in canopy structure after fire occurrence are exclusively
470 due to the canopy opening and consequently more penetration of photosynthetic radiation into the lower
471 canopy.

472 The model does not include neither characteristics related to resilience such as velocity, intensity
473 and duration of the burning (Hoffman et al., 2003; Rezende et al., 2005; Elias et al., 2013; Reis et al.,
474 2015) nor the representation of some tree morphological adaptation that confers to Cerrado species
475 resilience to fire occurrence, such as bark thickness. Thus, trees and grasses throughout the Amazon-
476 Cerrado border are equally exposed to the same fire intensity inside the grid cell, without fire resistance
477 differences. However, despite the limitations in the representation of resilience characteristics and
478 morphological attributes of fire resistance, our results show that simulated biomass is more close to
479 observed biomass in Cerrado areas when the fire module is activated (Figure 5). An improvement in
480 distribution of biomes along the simulated transition area is also observed (Figure 6g-i), highlighting
481 fire as an essential factor to represent the Amazonia-Cerrado border.

482 This study shows an improvement in the correlations between simulated and observed AGB
483 when compared to previous modeling studies, regardless of treatment, with correlation coefficients
484 usually above 0.80 for the transects, except for T5, for which the correlation coefficient value is usually
485 below 0.5 (Table 7). Senna et al. (2009) found 0.20 as maximum correlation coefficient between
486 simulated and observed ABG while Castanho et al. (2013) showed 0.80 for Amazonia domain. From
487 Figure 5, it is clear that CV, F and P limitation in the transition zone reduce the AGB, causing the

simulated data to approach the observed data. However, the inclusion of these effects is still insufficient to represent the correct distribution of the vegetation types throughout the Amazon-Cerrado border (Figure 6L). In our interpretation, this means that other important factors are still missing from the simulation, especially in T5, where soils are rocky and shallow. A better spatial representation of soil physical properties, including shallow rocky soils, as well as spatially varying physiological parameterizations of the vegetation such as carbon allocation, deciduousness of vegetation, residence time and tree structure that may discern thick from thin trees, are probably needed to improve the simulations, in particular in the northern and southern extremes of the border (T1 and T5).

In addition, literature shows that in the transition area, soils are very different than Amazon soils, and that essential proprieties for modeling are peculiar (Silva et al., 2006; Vourlitis et al., 2013; Dias et al. 2015). For example, Dias et al. (2015) recently showed that the pedological functions normally used by DGVMs may underestimate the saturated hydraulic conductivity (K_s) by >99%, transforming a well-drained soil with $K_s = 1.5.10^{-4}$ $m.s^{-1}$ (540 $mm.h^{-1}$) in reality into an impervious brick with $K_s = 3.3.10^{-7}$ $m.s^{-1}$ (1.2 $mm.h^{-1}$) in the model.

For all transects, the AGB curves have similar patterns (Figure 5); the smaller difference is observed between CA+PC and CV+PG curves, while the larger difference is when fire is present. The effect of P limitation appears as an effect of intermediate magnitude, reducing the AGB by more than the effect of inter-annual climate variability. In the east, it is observed that there is little or no difference among AGB simulated by CA+PC, CV+PC and CV+PG, revealing that inter-annual climate variability and P have smaller influence in the AGB. However, in the east of T2, T3 and T4, fire is the factor that

adjusts the simulated to the observed data (Figure 5), differently than the grid points in the West, where CV+PG is a better proxy between observed and simulated data.

Such conditions are interesting because they reflect the different mechanisms that regulate the structure of these ecosystems and probably the phytophysiognomies distribution. For example, P limitation seems to be the factor that improves simulated AGB in regions where the predominant vegetation type is the tropical rainforest. Fire, on the other hand, improves the AGB in grid points where the Cerrado occurs. Moreover, important factors such as productivity partitioning into leaves, roots and wood carbon pools are assumed to be fixed in space and time within a given PFT, neglecting the natural capacity of transitional forests to adapt itself and to adjust their metabolism to local environmental conditions (Senna et al., 2009). In years of severe drought, or under frequent fire occurrence, transitional forests could prioritize the stock of carbon in fine roots instead of the basal or leaf increment to maximize access to available water, make hydraulic redistribution of soil moisture to maintain the greenness and photosynthesis rates, or increase the capacity to resprout after fire occurrence (Hoffman et al., 2003; Brando et al., 2008). Brando et al. (2008) found high sensitivity in carbon allocation for eastern Amazon basin trees, which reduced wood production by 13-60% in response to an artificial drought. Although in INLAND soil moisture can reduce the photosynthetic rates during the months of lower rainfall, it does not dynamically change the allocation rates, exposing the PFTs in these areas to severe water stress and underestimating the AGB, such as in the west of T1 (Figure 5a).

T2, T3 and T4, located in the central part of the Amazon-Cerrado transition, showed the highest average correlations between observed and simulated data (Table 7). For these transects, INLAND seems to be able to capture the high variability of AGB gradient.

At T5, located at the south of the transition, the average correlations were low for all treatments, indicating that INLAND has difficulty to represent the AGB gradient there (Table 7). However, it captures the lower AGB as compared to the northern ones. In this region, the vegetation is characterized by a wide diversity of physiognomies, which varies with other preponderant factors, such as lithology, soil depth, topography and fertility. The observed data also showed high AGB variability, indicating that there are changes in the vegetation structure, featuring medium-sized and small vegetation types on different soil types. In INLAND, however, features such as lithology and water-table depth are not considered due to the complexity of its representation on the large scale, limiting the representation of a heterogeneous environment throughout the transition.

Patterns of vegetation distribution along the Amazon-Cerrado border exist are influenced not only by inter-annual climate variability, P limitation, and fire, but also by the ecophysiological parameters. Additional field experiments are needed to understand the relationship between currently fixed parameters (such as carbon allocation, residence time, and deciduousness, among others) to the environmental conditions and soil proprieties.

Another point to discuss is that the model simulates, in a few pixels in southeastern Cerrado, very robust simulations of the presence of savanna and grassland even in the absence of fire (Figure 6A-F and 6a-f). This is, in our view, a result of the intense water and heat stress in this region. In the Brazilian Cerrado, the high temperatures (> 35 °C) combined to the dry season duration (as long as 6

548 months with little or no rain) exposes the vegetation to a severely stressed situation, so that a low
549 biomass, low LAI vegetation may exist without the need of a frequent disturbance.
550

551 **5 Conclusions**

552 This is the first study that uses modeling to assess the influence of inter-annual climate
553 variability, fire occurrence and phosphorus limitation to represent the Amazon-Cerrado border. This
554 study shows that, although the model forced by a climatological database is able to simulate basic
555 characteristics of the Amazon-Cerrado transition, the addition of factors such as inter-annual climate
556 variability, phosphorus limitation and fire gradually improves simulated vegetation types. These effects
557 are not homogeneous along the latitudinal/longitudinal gradient, which makes the adequate simulation
558 of biomass challenging in some places along the transition. Based on the F-statistic in Tables 3, 4 and 5,
559 this work shows that fire is in the main determinant factor of the changes in vegetation structure (LAI,
560 AGB) along the transition. The nutrient limitation is second in magnitude, stronger than the effect of
561 inter-annual climate variability.

562 Overall, although INLAND typically simulates more than 80% of the variability of biomass in
563 the transition zone, in many places the biomass is clearly not well simulated. Situations for clearly wet
564 or markedly dry climate conditions were well simulated, but the simulations are generally poor for
565 transitional areas where the environment selected physiognomies that have an intermediate behavior, as
566 is the case of the transitional forests in northern Tocantins and Mato Grosso.

567 There are evidences that the inclusion of spatially explicit parameters such as woody biomass
568 residence time, maximum carboxylation capacity (V_{max}), and NPP allocation to wood may improve

Amazon rainforest AGB simulation by DGVMs (Castanho et al., 2013). However, in the transition, the lack of field parameters measured limits the inclusion of the variability of these biophysical parameters in DGVMs. Additional field work and compilation of existing ones are necessary to obtain physiological and structural parameters through the Amazon-Cerrado border to establish numerical relationships between soil, climate and vegetation. With the help of these data, the vegetation dynamic models will be able to correctly simulate current patterns and future changes in vegetation considering climate change scenarios. In addition, it is also needed to include not only the spatial variability, but also temporal variability in physiological parameters of vegetation, allowing a more realistic simulation of the soil-climate-vegetation relationship. Finally, our results reinforce the importance and need of the DGVMs to incorporate the nutrient limitation and fire occurrence to simulate the Amazon-Cerrado border position.

6 Acknowledgements

We gratefully thank the Brazilian agencies FAPEMIG and CAPES for their financial support. Atul K Jain is funded by the U.S. National Science Foundation (NSF-AGS- 12-43071).

7 References

Andreoli, R. V., Ferreira de Souza, R. A., Kayano, M. T. and Candido, L. A.: Seasonal anomalous rainfall in the central and eastern Amazon and associated anomalous oceanic and atmospheric patterns, Int. J. Climatol., 32(8), 1193–1205, doi:10.1002/joc.2345, 2012.

Aragão, L. E. O. C., Malhi, Y., Metcalfe, D. B., Silva-Espejo, J. E., Jiménez, E., Navarrete, D., Almeida, S., Costa, A. C. L., Salinas, N., Phillips, O. L., Anderson, L. O., Baker, T. R., Goncalvez, P.

H., Huamán-Ovalle, J., Mamani-Solórzano, M., Meir, P., Monteagudo, A., Peñuela, M. C., Prieto, A., Quesada, C. A., Rozas-Dávila, A., Rudas, A., Silva Junior, J. A. and Vásquez, R.: Above- and below-ground net primary productivity across ten Amazonian forests on contrasting soils, Biogeosciences, 6, 2441–2488, doi:10.5194/bgd-6-2441-2009, 2009.

Arora, V. K. and Boer, G. J.: Fire as an interactive component of dynamic vegetation models, J. Geophys. Res, 110, doi:10.1029/2005JG000042, 2005

Balch, J. K., Brando, P. M., Nepstad, D. C., Coe, M. T., Silvério, D., Massad, T. J., Davidson, E. A., Lefebvre, P., Oliveira-Santos, C., Rocha, W., Cury, R. T. S., Parsons, A. and Carvalho, K. S.: The Susceptibility of Southeastern Amazon Forests to Fire: Insights from a Large-Scale Burn Experiment, Bioscience, 65(9), 893–905, doi:10.1093/biosci/biv106, 2015.

Beguería, S., Vicente-Serrano, S. M., Tomás-Burguera, M. and Maneta, M.: Bias in the variance of gridded data sets leads to misleading conclusions about changes in climate variability. Int. J. Climatol., 36: 3413–3422. doi:10.1002/joc.4561, 2016.

Betts, R. A., Cox, P. M., Collins, M., Harris, P. P., Huntingford, C. and Jones, C. D.: The role of ecosystem-atmosphere interactions in simulated Amazonian precipitation decrease and forest dieback under global climate warming, Theor. Appl. Climatol., 78, 157–175, doi:10.1007/s00704-004-0050-y, 2004.

Bonan, G. B.: Forests and climate change: forcings, feedbacks, and the climate benefits of forests, Science, 320(5882), 1444–1449, doi:10.1126/science.1155121, 2008.

Bond, W. J., Woodward, F. I. and Midgley, G. F.: The global distribution of ecosystems in a world without fire, New Phytol., 165(2), 525–538, doi:10.1111/j.1469-8137.2004.01252.x, 2005.

611 Botta, A. and Foley, J. A.: Effects of climate variability and disturbances on the Amazonian
612 terrestrial ecosystems dynamics, Global Biogeochem. Cycles, 16(4), doi:10.1029/2000GB001338,
613 2002.
614 Brando, P. M., Nepstad, D. C., Davidson, E. A., Trumbore, S. E., Ray, D. and Camargo, P.:
615 Drought effects on litterfall, wood production and belowground carbon cycling in an Amazon forest:
616 results of a throughfall reduction experiment, Philos. Trans. R. Soc. Lond. B. Biol. Sci., 363(1498),
617 1839–48, doi:10.1098/rstb.2007.0031, 2008.
618 Castanho, A. D. A., Coe, M. T., Costa, M. H., Malhi, Y., Galbraith, D. and Quesada, C. A.:
619 Improving simulated Amazon forest AGB and productivity by including spatial variation in biophysical
620 parameters, Biogeosciences, 10(4), 2255–2272, doi:10.5194/bg-10-2255-2013, 2013.
621 Couto-Santos, F. R., Luizão, F. J. and Carneiro Filho, A.: The influence of the conservation
622 status and changes in the rainfall regime on forest-savanna mosaic dynamics in Northern Brazilian
623 Amazonia, Acta Amaz., 44(2), 197–206, 2014.
624 Cox, P. M., Betts, R. A., Jones, C. D., Spall, S. A. and Totterdell, I. J.: Acceleration of global
625 warming due to carbon-cycle feedbacks in a coupled climate model, Nature, 408(November), 184–187,
626 doi:10.1038/35041539, 2000.
627 Cox, P. M., Betts, R. A., Collins, M., Harris, P. P., Huntingford, C. and Jones, C. D.: Amazonian
628 forest dieback under climate-carbon cycle projections for the 21st century, Theor. Appl. Climatol., 78,
629 137–156, doi:10.1007/s00704-004-0049-4, 2004.
630 Dajoz, R.: Princípios de ecologia, 7º edição, Artmed, Porto Alegre, RS, Brazil 519pp, 2005.

631 Dantas, V. L., Batalha, M. A. and Pausas, J. G.: Fire drives functional thresholds on the savanna-
632 forest transition, Ecology, 94(11), 2454–2463, doi:10.1890/12-1629.1, 2013.
633 Davidson, E. A., Carvalho, C. J.R., Vieira, I. C. G., Figueiredo, R. D. O., Moutinho, P., Ishida,
634 F.Y., Santos, M. T.P., Guerrero, J.B., Kalif, K. and Sabá, R.T.: Nitrogen and Phosphorus Limitation of
635 Biomass Growth in a Tropical Secondary Forest, Ecol. Appl., 14(4), 150–163, doi:10.1890/01-6006,
636 2004.
637 Dias, L. C. P., Macedo, M. N., Costa, M. H., Coe, M. T. and Neill, C.: Effects of land cover
638 change on evapotranspiration and streamflow of small catchments in the Upper Xingu River Basin,
639 Central Brazil, J. Hydrol. Reg. Stud., 4, 108–122, doi:10.1016/j.ejrh.2015.05.010, 2015.
640 Elias, F., Marimon, B. S., Matias, S. R. A., Forsthofer, M., Morandi, P. S. and Marimon-junior,
641 B. H.: Dinâmica da distribuição espacial de populações arbóreas, ao longo de uma década, em cerradão
642 na transição Cerrado-Amazônia, Mato Grosso, Biota Amaz., 3, 1–14, 2013.
643 Favier, C., Chave, J., Fabing, A., Schwartz, D. and Dubois, M. A.: Modelling forest-savanna
644 mosaic dynamics in man-influenced environments: Effects of fire, climate and soil heterogeneity, Ecol.
645 Modell., 171, 85–102, doi:10.1016/j.ecolmodel.2003.07.003, 2004.
646 Foley, J. A., Prentice, I. C., Ramankutty, N., Levis, S., Pollard, D., Sitch, S. and Haxeltine, A.:
647 An integrated biosphere model of land surface processes, terrestrial carbon balance, and vegetation
648 dynamics, Global Biogeochem. Cycles, 10, 603, doi:10.1029/96GB02692, 1996.
649 Foley, J. A., Botta,A., Coe, M. T. and Costa, M. H.: El Niño–Southern oscillation and the
650 climate, ecosystems and rivers of Amazonia, Global Biogeochem. Cycles, 16(4), 1132,
651 doi:10.1029/2002GB001872, 2002.

652 Goedert, W: Solos do Cerrado: Tecnologias e Estratégias de Manejo, Empresa Brasileira de
653 Pesquisa Agropecuária (EMBRAPA), Brasília, DF, Brasil. 422pp., 1986.
654 Hansen, M. C. and Reed, B.: A comparison of the IGBP DISCover and University of Maryland
655 1km global land cover products, Int. J. Remote Sens., 21, 1365–1373, doi:10.1080/014311600210218,
656 2000.
657 Harris, I., Jones, P. D., Osborn, T. J. and Lister, D. H.: Updated high-resolution grids of monthly
658 climatic observations - the CRU TS3.10 Dataset, Int. J. Climatol., 34(3), 623–642,
659 doi:10.1002/joc.3711, 2014.
660 Hilker, T., Lyapustin, A. I., Tucker, C. J., Hall, F. G., Myneni, R. B., Wang, Y., Bi, J., Mendes
661 de Moura, Y. and Sellers, P. J.: Vegetation dynamics and rainfall sensitivity of the Amazon., Proc. Natl.
662 Acad. Sci. U. S. A., 111(45), 16041–6, doi:10.1073/pnas.1404870111, 2014.
663 Hirota, M., Nobre, C., Oyama, M. D. and Bustamante, M. M. C.: The climatic sensitivity of the
664 forest, savanna and forest-savanna transition in tropical South America, New Phytol., 187, 707–719,
665 doi:10.1111/j.1469-8137.2010.03352.x, 2010.
666 Hoffmann, W. A., B. Orthen, and P. K. V. Nascimento.: Comparative fire ecology of tropical
667 savanna and forest trees, Functional Ecology, 17:720–726, 2003.
668 Hoffmann, W.A., Adasme, R., Haridasan, M., Carvalho, M., Geiger, E.L., Pereira, M.A.B.,
669 Gotsch, S.G., and Franco, A.C.:Tree topkill, not mortality, governs the dynamics of alternate stable
670 states at savanna-forest boundaries under frequent fire in central Brazil, Ecology, 90, 1326–1337, 2009.
671 Hoffmann, W. A., Geiger, E. L., Gotsch, S. G., Rossatto, D. R., Silva, L. C. R., Lau, O. L.,
672 Haridasan, M. and Franco, A. C.: Ecological thresholds at the savanna-forest boundary: How plant

673 traits, resources and fire govern the distribution of tropical biomes, Ecol. Lett., 15, 759–768,
674 doi:10.1111/j.1461-0248.2012.01789.x, 2012.
675 House, J. I., Archer, S., Breshears, D. D. and Scholes, R. J.: Conundrums in mixed woody-
676 herbaceous plant systems, J. Biogeogr., 30, 1763–1777, doi:10.1046/j.1365-2699.2003.00873.x, 2003.
677 IBGE.: Manual Técnico da Vegetação Brasileira (Manuais Técnicos em Geociências n. 1),
678 Fundação Instituto Brasileiro de Geografia e Estatística (IBGE), Rio de Janeiro, RJ, Brasil. 92pp., 1992.
679 IBGE.: Mapa da Vegetação do Brasil, Fundação Instituto Brasileiro de Geografia e Estatística
680 (IBGE), Rio de Janeiro, RJ, Brazil, Map, 2004.
681 Klink, C. A. and Machado, R. B.: Conservation of the Brazilian Cerrado, Conserv. Biol., 19(3),
682 707–713, doi:10.1111/j.1523-1739.2005.00702.x, 2005.
683 Kucharik, C. J., Foley, J. A., Delire, C., Fisher, V. A., Coe, M. T., Lenters, J. D., Young-
684 Molling, C., Ramankutty, N., Norman, J. M. and Gower, S. T.: Testing the performance of a Dynamic
685 Global Ecosystem Model: Water balance, carbon balance, and vegetation structure, Global
686 Biogeochem. Cycles, 14(3), 795–825, doi:10.1029/1999GB001138, 2000.
687 Lee, J. E., Frankenberg, C., van der Tol, C., Berry, J. A., Guanter, L., Boyce, C. K., Fisher, J. B.,
688 Morrow, E., Worden, J. R., Asefi, S., Badgley, G. and Saatchi, S.: Forest productivity and water stress
689 in Amazonia: observations from GOSAT chlorophyll fluorescence, Proc. R. Soc. B Biol. Sci.,
690 280(1761), 20130171–20130171, doi:10.1098/rspb.2013.0171, 2013.
691 Lehmann, C. E. R., Archibald, S. A., Hoffmann, W. A. and Bond, W. J.: Deciphering the
692 distribution of the savanna biome, New Phytol., 191, 197–209, doi:10.1111/j.1469-8137.2011.03689.x,
693 2011.

694 Lehmann, C. E. R., Anderson, T. M., Sankaran, M., Higgins, S. I., Archibald, S., Hoffmann, W.
695 A., Hanan, N. P., Williams, R. J., Fensham, R. J., Felfili, J., Hutley, L. B., Ratnam, J., Jose, J. S.,
696 Montes, R., Franklin, D., Russell-Smith, J., Ryan, C. M., Durigan, G., Hiernaux, P., Haidar, R.,
697 Bowman, D. M. J. S., and Bond, W. J.: Savanna Vegetation-Fire-Climate Relationships Differ Among
698 Continents, Science, 343 (January), 548–553, doi:10.1126/science.1247355, 2014.
699 Long, W., Yang, X. and Donghai, L.: Patterns of species diversity and soil nutrients along a
700 chronosequence of vegetation recovery in Hainan Island, South China, Ecol. Res., 2012.
701 Malhi, Y., Aragão, L. E. O. C., Metcalfe, D. B., Paiva, R., Quesada, C. A., Almeida, S.,
702 Anderson, L., Brando, P., Chambers, J. Q., da Costa, A. C. L., Hutyra, L. R., Oliveira, P., Patiño, S.,
703 Pyle, E. H., Robertson, A. L. and Teixeira, L. M.: Comprehensive assessment of carbon productivity,
704 allocation and storage in three Amazonian forests, Glob. Chang. Biol., 15, 1255–1274,
705 doi:10.1111/j.1365-2486.2008.01780.x, 2009.
706 Marengo, J. A.: Interdecadal variability and trends of rainfall across the Amazon basin, Theor.
707 Appl. Climatol., 78(1–3), 79–96, doi:10.1007/s00704-004-0045-8, 2004.
708 Marimon Junior, B. H. and Haridasan, M.: Comparação da vegetação arbórea e características
709 edáficas de um cerradão e um cerrado sensu stricto em áreas adjacentes sobre solo distrófico no leste de
710 Mato Grosso, Brasil, Acta Bot. Brasilica, 19(4), 913–926, doi:10.1590/S0102-33062005000400026,
711 2005.
712 Marimon, B. S., Lima, E. S., Duarte, T. G., Chieregatto, L. C., Ratter, J. A.: Observations on the
713 vegetation of northeastern Mato Grosso, Brazil. IV. An analysis of the Cerrado-Amazonian Forest
714 ecotone, Edinburgh Journal of Botany, 63, 323–341, doi: 10.1017/S0960428606000576, 2006.

715 Marimon, B. S., Marimon-Junior, B. H., Feldpausch, T. R., Oliveira-Santos, C., Mews, H. A.,
716 Lopez-Gonzalez, G., Lloyd, J., Franczak, D. D., de Oliveira, E. A., Maracahipes, L., Miguel, A., Lenza,
717 E. and Phillips, O. L.: Disequilibrium and hyperdynamic tree turnover at the forest–cerrado transition
718 zone in southern Amazonia, Plant Ecol. Divers., 7(1–2), 281–292, doi:10.1080/17550874.2013.818072,
719 2014.
720 Mercado, L. M., Patino, S., Domingues, T. F., Fyllas, N. M., Weedon, G. P., Sitch, S., Quesada,
721 C. A., Phillips, O. L., Aragao, L. E. O. C., Malhi, Y., Dolman, A. J., Restrepo-Coupe, N., Saleska, S. R.,
722 Baker, T. R., Almeida, S., Higuchi, N. and Lloyd, J.: Variations in Amazon forest productivity
723 correlated with foliar nutrients and modelled rates of photosynthetic carbon supply, Philos. Trans. R.
724 Soc. Lond. B. Biol. Sci., 366(1582), 3316–3329, doi:10.1098/rstb.2011.0045, 2011.
725 Morandi, P.S., Marimon-Junior, B. H., Oliveira, E. A., Reis, S. M. A., Valadão, M. B. X.,
726 Forsthofer, M., Passos, F. B., Marimon, B. S.: Vegetation Succession in the Cerrado-Amazonian Forest
727 Transition Zone of Mato Gross State, Brazil, Edinburgh Journal of Botany, 73, 83-93, doi:
728 10.1017/S096042861500027X, 2016.
729 Moreno, M. I. C., Schiavini, I. and Haridasan, M.: Fatores edáficos influenciando na estrutura de
730 fitofisionomias do cerrado, Caminhos da Geogr., 9(25), 173–194, 2008.
731 Murphy, B. P. and Bowman, D. M. J. S.: What controls the distribution of tropical forest and
732 savanna?, Ecol. Lett., 15, 748–758, doi:10.1111/j.1461-0248.2012.01771.x, 2012.
733 Myers, N., Fonseca, G. A B., Mittermeier, R. A, Fonseca, G. A. B. and Kent, J.: Biodiversity
734 hotspots for conservation priorities, Nature, 403(6772), 853–858, doi:10.1038/35002501, 2000.

735 Nardoto, G. B., Bustamante, M. M. C., Pinto, A. S. and Klink, C. A. Nutrient use efficiency at
736 ecosystem and species level in savanna areas of Central Brazil and impacts of fire, J. Trop. Ecol., 22,
737 191–201, doi:10.1017/S0266467405002865, 2006.
738 Nogueira, E. M., Yanai, A. M., Fonseca, F. O. and Fearnside, P. M.: Carbon stock loss from
739 deforestation through 2013 in Brazilian Amazonia, Glob. Chang. Biol., doi:10.1111/gcb.12798, 2015.
740 Nunes, E. L., Costa, M. H., Malhado, A. C. M., Dias, L. C. P., Vieira, S. A., Pinto, L. B. and
741 Ladle, R. J.: Monitoring carbon assimilation in South America's tropical forests: Model specification
742 and application to the Amazonian droughts of 2005 and 2010, Remote Sens. Environ., 117, 449–463,
743 doi:10.1016/j.rse.2011.10.022, 2012.
744 Oliveira, B., Marimon-Junior, B. H., Mews, H. A., Valadão, M. B. X., Marimon, B. S.:
745 Unraveling the ecosystem functions in the Amazonia–Cerrado transition: evidence of hyperdynamic
746 nutrient cycling, Plant Ecol., 218(2), 225–239, doi:10.1007/s11258-016-0681-y, 2017.
747 Oyama, M. D. and Nobre, C. A.: A new climate-vegetation equilibrium state for Tropical South
748 America, Geophys. Res. Lett., 30(23), 10–13, doi:10.1029/2003GL018600, 2003.
749 Parton, W. J., Scurlock, J. M. O., Ojima, D. S., Gilmanov, T. G., Scholes, R. J., Schimel, D. S.,
750 Kirchner, T., Menaut, J.-C., Seastedt, T., Garcia Moya, E., Kamnalrut, A. and Kinyamario, J. I.:
751 Observations and modeling of AGB and soil organic matter dynamics for the grassland biome
752 worldwide, Global Biogeochem. Cycles, 7, 785, doi:10.1029/93GB02042, 1993.
753 Pereira, M. P. S., Malhado, A. C. M. and Costa, M. H.: Predicting land cover changes in the
754 Amazon rainforest: An ocean-atmosphere-biosphere problem, Geophys. Res. Lett., 39(9),
755 doi:10.1029/2012GL051556, 2012.

Pires, G. F. and Costa, M. H.: Deforestation causes different subregional effects on the Amazon bioclimatic equilibrium, Geophys. Res. Lett., 40(14), 3618–3623, doi:10.1002/grl.50570, 2013.

Quesada, C. A., Lloyd, J., Schwarz, M., Baker, T. R., Phillips, O. L., Patiño, S., Czimczik, C., Hodnett, M. G., Herrera, R., Arneth, A., Lloyd, G., Malhi, Y., Dezzeo, N., Luizão, F. J., Santos, A. J. B., Schmerler, J., Arroyo, L., Silveira, M., Priante Filho, N., Jimenez, E. M., Paiva, R., Vieira, I., Neill, D. A., Silva, N., Peñuela, M. C., Monteagudo, A., Vásquez, R., Prieto, A., Rudas, A., Almeida, S., Higuchi, N., Lezama, A. T., López-González, G., Peacock, J., Fyllas, N. M., Alvarez Dávila, E., Erwin, T., di Fiore, A., Chao, K. J., Honorio, E., Killeen, T., Peña Cruz, A., Pitman, N., Núñez Vargas, P., Salomão, R., Terborgh, J. and Ramírez, H.: Regional and large-scale patterns in Amazon forest structure and function are mediated by variations in soil physical and chemical properties, Biogeosciences Discuss., 6, 3993–4057, doi:10.5194/bgd-6-3993-2009, 2009.

Quesada, C. A., Lloyd, J., Anderson, L. O., Fyllas, N. M., Schwarz, M. and Czimczik, C. I.: Soils of Amazonia with particular reference to the RAINFOR sites, Biogeosciences, 8, 1415–1440, doi:10.5194/bg-8-1415-2011, 2011.

Quesada, C. A., Phillips, O. L., Schwarz, M., Czimczik, C. I., Baker, T. R., Patiño, S., Fyllas, N. M., Hodnett, M. G., Herrera, R., Almeida, S., Alvarez Dávila, E., Arneth, A., Arroyo, L., Chao, K. J., Dezzeo, N., Erwin, T., Di Fiore, A., Higuchi, N., Honorio Coronado, E., Jimenez, E. M., Killeen, T., Lezama, A. T., Lloyd, G., Löpez-González, G., Luizão, F. J., Malhi, Y., Monteagudo, A., Neill, D. A., Núñez Vargas, P., Paiva, R., Peacock, J., Peñuela, M. C., Peña Cruz, A., Pitman, N., Priante Filho, N., Prieto, A., Ramírez, H., Rudas, A., Salomão, R., Santos, A. J. B., Schmerler, J., Silva, N., Silveira, M., Vásquez, R., Vieira, I., Terborgh, J. and Lloyd, J.: Basin-wide variations in Amazon forest structure and

function are mediated by both soils and climate, Biogeosciences, 9(6), 2203–2246, doi:10.5194/bg-9-2203-2012, 2012.

Reis, S. M., Marimon, B. S., Marimon Junior, B.-H., Gomes, L., Morandi, P. S., Freire, E. G. and Lenza, E.: Resilience of savanna forest after clear-cutting in the Cerrado-Amazon transition zone, Bioscience, 31(5), 1519–1529, doi:10.14393/BJ-v31n5a2015-26368, 2015.

Restrepo-Coupe, N., da Rocha, H. R., Hutyra, L. R., da Araujo, A. C., Borma, L. S., Christoffersen, B., Cabral, O. M. R., de Camargo, P. B., Cardoso, F. L., da Costa, A. C. L., Fitzjarrald, D. R., Goulden, M. L., Kruijt, B., Maia, J. M. F., Malhi, Y. S., Manzi, A. O., Miller, S. D., Nobre, A. D., von Randow, C., S, L. D. A., Sakai, R. K., Tota, J., Wofsy, S. C., Zanchi, F. B. and Saleska, S. R.: What drives the seasonality of photosynthesis across the Amazon basin? A cross-site analysis of eddy flux tower measurements from the Brazil flux network, Agric. For. Meteorol., 182–183, 128–144, doi:10.1016/j.agrformet.2013.04.031, 2013.

Rezende, A. V, Sanquetta, C. R. and Filho, F. A.: Efeito do desmatamento no estabelecimento de espécies lenhosas em um cerrado Sensu stricto, Floresta, 35, 69–88, 2005.

Ribeiro, J. F. and Walter, B. M. T.: As Principais Fitofisionomias do bioma Cerrado, in Cerrado: ecologia e flora, pp. 153–212., 2008.

Rocha, H. R. da, Goulden, M. L., Miller, S. D., Menton, M. C., Pinto, L. D. V. O., De Freitas, H. C. and Figueira, A. M. E. S.: Seasonality of water and heat fluxes over a tropical forest in eastern Amazonia, Ecol. Appl., 14(4 SUPPL.), doi:10.1890/02-6001, 2004.

Roy, S. B. and Avissar, R.: Impact of land use/land cover change on regional hydrometeorology in Amazonia, J. Geophys. Res., 107(D20), 1–12, doi:10.1029/2000JD000266, 2002.

798 Saatchi, S., Houghton, R. A., Dos Santos Alvalá, R. C., Soares, J. V. and Yu, Y.: Distribution of
799 aboveground live AGB in the Amazon basin, Glob. Chang. Biol., 13(4), 816–837, doi:10.1111/j.1365-
800 2486.2007.01323.x, 2007.
801 Salazar, L. F., Nobre, C. A. and Oyama, M. D.: Climate change consequences on the biome
802 distribution in tropical South America, Geophys. Res. Lett., 34(April), 2–7,
803 doi:10.1029/2007GL029695, 2007.
804 Senna, M. C. A., Costa, M. H., Pinto, L. I.C., Imbuzeiro, H. M. A., Diniz, L. M. F. and Pires, G.
805 F.: Challenges to reproduce vegetation structure and dynamics in Amazonia using a coupled climate-
806 biosphere model, Earth Interact., 13(11), doi:10.1175/2009EI281.1, 2009.
807 Shukla, J., Nobre, C. and Sellers, P.: Amazon deforestation and climate change, Science, 247,
808 1322–1325, doi:10.1126/science.247.4948.1322, 1990.
809 Silva, J. F., Fariñas, M. R., Felfili, J. M. and Klink, C. A.: Spatial heterogeneity, land use and
810 conservation in the cerrado region of Brazil, in Journal of Biogeography, vol. 33, pp. 536–548., 2006.
811 Silvério, D. V, Brando, P. M., Balch, J. K., Putz, F. E., Nepstad, D. C., Oliveira-Santos, C. and
812 Bustamante, M. M. C.: Testing the Amazon savannization hypothesis: fire effects on invasion of a
813 neotropical forest by native cerrado and exotic pasture grasses, Philos. Trans. R. Soc. Lond. B. Biol.
814 Sci., 368, 20120427, doi:10.1098/rstb.2012.0427, 2013.
815 Smith, B., Wärlind, D., Arneth, A., Hickler, T., Leadley, P., Siltberg, J. and Zaehle, S.:
816 Implications of incorporating N cycling and N limitations on primary production in an individual-based
817 dynamic vegetation model, Biogeosciences, 11(7), 2027–2054, doi:10.5194/bg-11-2027-2014, 2014.

Thompson, S. L. and Pollard, D.: A global climate model (GENESIS) with a land-surface transfer scheme (LSX). Part I: present climate simulation, J. Clim., 8, 732–761, doi:10.1175/1520-0442(1995)008<0732:AGCMWA>2.0.CO;2, 1995.

Torello-Raventos, M., Feldpausch, T., Veenendaal, E., Schrodt, F., Saiz, G., Domingues, T., Djagbletey, G., Ford, A., Kemp, J., Marimon, B., Hur Marimon Junior, B., Lenza, E., Ratter, J., Maracahipes, L., Sasaki, D., Sonké, B., Zapfack, L., Taedoumg, H., Villarroel, D., Schwarz, M., Quesada, C., Yoko Ishida, F., Nardoto, G., Affum-Baffoe, K., Arroyo, L., Bowman, D., Compaore, H., Davies, K., Diallo, A., Fyllas, N., Gilpin, M., Hien, F., Johnson, M., Killeen, T., Metcalfe, D., Miranda, H., Steininger, M., Thomson, J., Sykora, K., Mougin, E., Hiernaux, P., Bird, M., Grace, J., Lewis, S., Phillips, O. and Lloyd, J.: On the delineation of tropical vegetation types with an emphasis on forest/savanna transitions, Plant Ecol. Divers., 6, 101–137, doi:10.1080/17550874.2012.76281, 2013.

Valadão, M. B. X., Marimon-Junior, B. H., Oliveira, B., Lúcio, N. W., Souza, M. G. R., Marimon, B. S.: AGB hyperdynamic as a key modulator of forest self-maintenance in dystrophic soil at Amazonia-Cerrado transition. Scientia Forestalis, 44, 475-485, 2016.

Veenendaal, E. M., Torello-Raventos, M., Feldpausch, T. R., Domingues, T. F., Gerard, F., Schrodt, F., Saiz, G., Quesada, C. A., Djagbletey, G., Ford, A., Kemp, J., Marimon, B. S., Marimon-Junior, B. H., Lenza, E., Ratter, J. A., Maracahipes, L., Sasaki, D., Sonk, B., Zapfack, L., Villarroel, D., Schwarz, M., Yoko Ishida, F., Gilpin, M., Nardoto, G. B., Affum-Baffoe, K., Arroyo, L., Bloomfield, K., Ceca, G., Compaore, H., Davies, K., Diallo, A., Fyllas, N. M., Gignoux, J., Hien, F., Johnson, M., Mougin, E., Hiernaux, P., Killeen, T., Metcalfe, D., Miranda, H. S., Steininger, M., Sykora, K., Bird, M. I., Grace, J., Lewis, S., Phillips, O. L. and Lloyd, J.: Structural, physiognomic and above-ground AGB

variation in savanna-forest transition zones on three continents - How different are co-occurring savanna and forest formations?, Biogeosciences, 12(10), 2927–2951, doi:10.5194/bg-12-2927-2015, 2015.

Verberne, E. L. J., Hassink, J., De Willigen, P., Groot, J. J. R. and Van Veen, J. A.: Modelling organic matter dynamics in different soils, Netherlands J. Agric. Sci., 38, 221–238, 1990.

Vourlitis, G. L., de Lobo, F. A., Lawrence, S., de Lucena, I. C., Pinto, O. B., Dalmagro, H. J., Ortiz, C. E. and de Nogueira, J. S.: Variations in Stand Structure and Diversity along a Soil Fertility Gradient in a Brazilian Savanna (Cerrado) in Southern Mato Grosso, Soil Sci. Soc. Am. J., 77(4), 1370–1379, doi:10.2136/sssaj2012.0336, 2013.

Yang, X. and Post, W. M.: Phosphorus transformations as a function of pedogenesis: A synthesis of soil phosphorus data using Hedley fractionation method, Biogeosciences, 8, 2907–2916, doi:10.5194/bg-8-2907-2011, 2011.

Yang, X., Post, W. M., Thornton, P. E. and Jain, A.: The distribution of soil phosphorus for global biogeochemical modeling, Biogeosciences, 10, 2525–2537, doi:10.5194/bg-10-2525-2013, 2013.

Yang, X., Thornton, P. E., Ricciuto, D. M. and Post, W. M.: The role of phosphorus dynamics in tropical forests - A modeling study using CLM-CNP, Biogeosciences, 11, 1667–1681, doi:10.5194/bg-11-1667-2014, 2014.

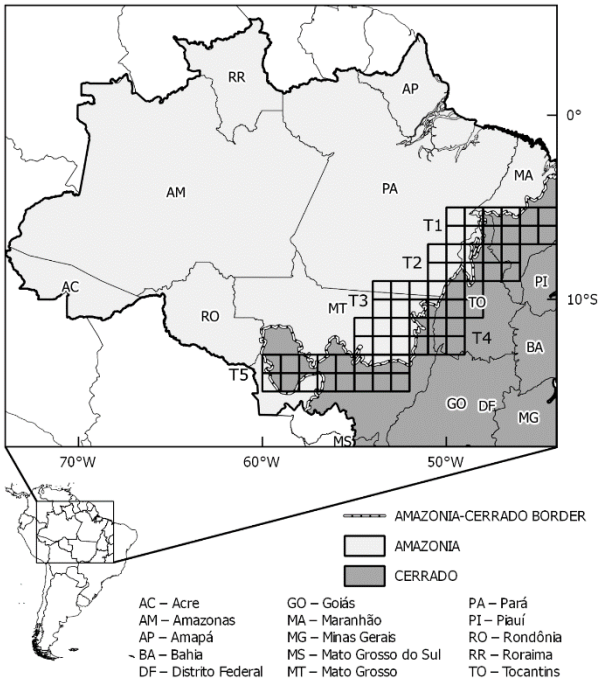

Figure 1. Delimitation of the study area Amazonia (in light gray) and Cerrado (in dark gray) (IBGE, 2004), and the location of five transects used in this work (from T1 to T5). The dashed line represents the border between biomes.

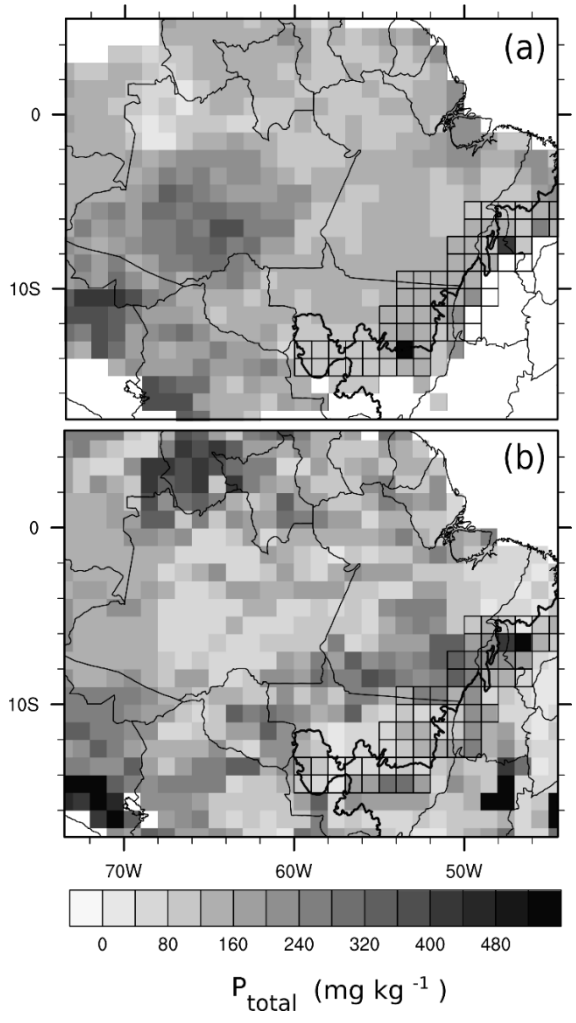

Figure 2. (a) Map of regional total P in the soil (PR), (b) Map of global total P in the soil (Yang et al., 2013) (PG).

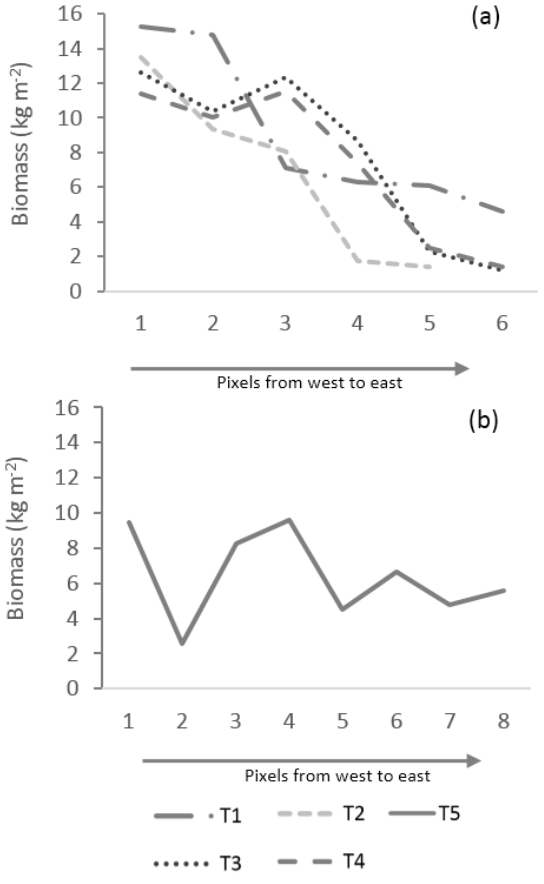

866

867 **Figure 3.** Average variations of AGB in pixels from West to East in the Amazonia-Cerrado transition

868 for transects T1, T2, T3 and T4 (a), and T5 (b).

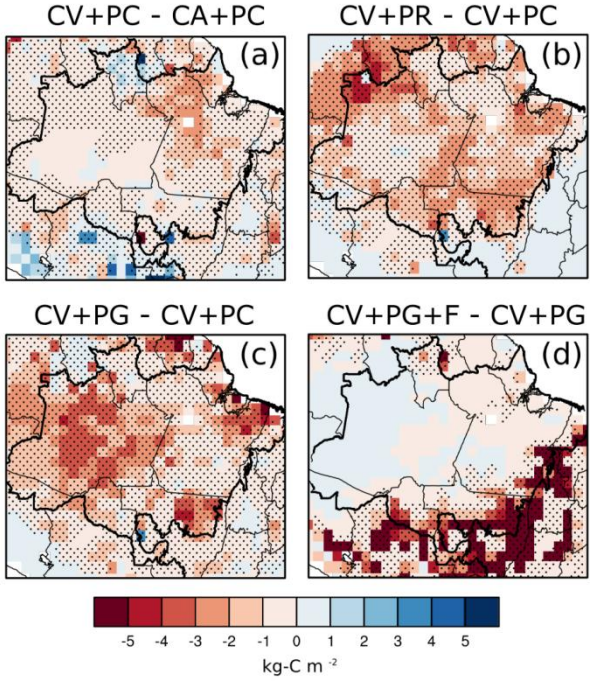

869

870 **Figure 4.** Effects of inter-annual climate variability (a), Regional P limitation (b), Global P limitation
871 (c), and fire (d) on AGB. The hatched areas indicate that the variables are significantly different
872 compared to the control simulation at the level of 95% according to the t-test. The thick black line is the
873 geographical limits of the biomes.

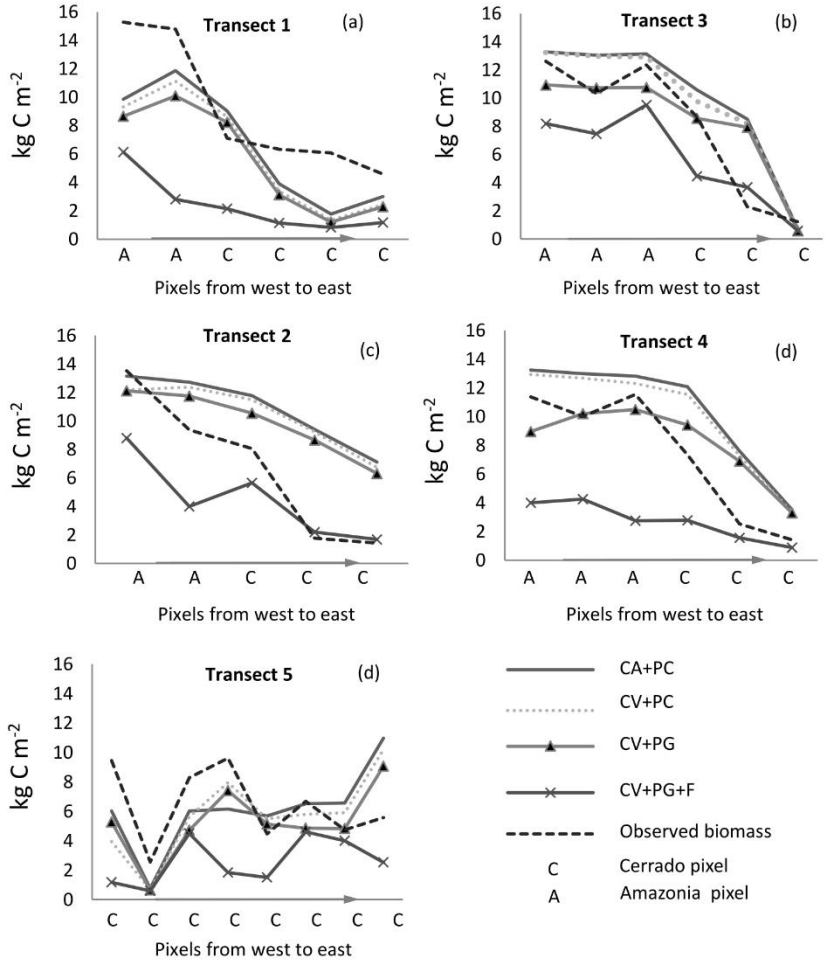

874

875 **Figure 5.** Average longitudinal AGB gradient in Amazonia-Cerrado transition simulated for T1 to T5
876 considering different combinations: observed data; seasonal climate control simulation (CA+PC); inter-
877 annual climate variability (CV+PC); inter-annual climate variability + global P limitation (CV+PG);
878 and inter-annual climate variability + P + fire occurrence (CV+PG+F).

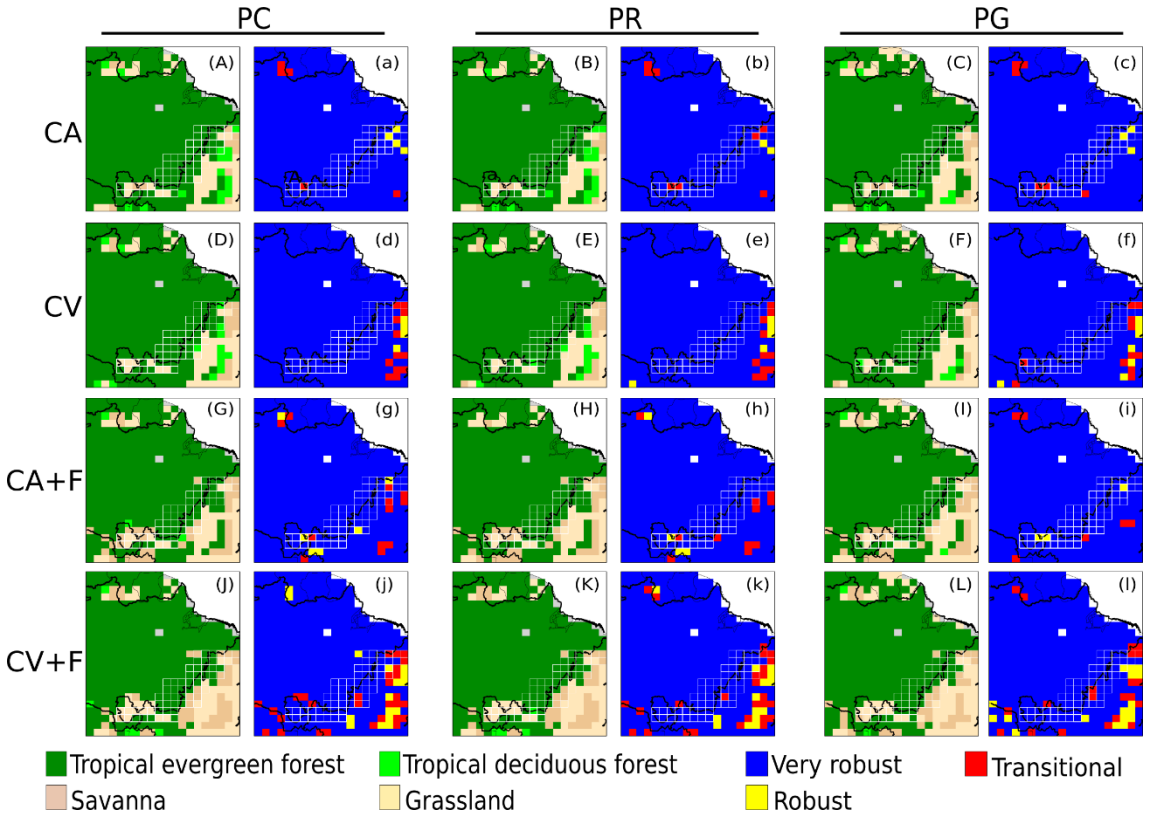

Figure 6. Results for the dominant vegetation cover simulated by INLAND for the different treatments (A-L) and a metric of variability of results (a-l). Simulations are considered very robust if the dominant vegetation agrees on 9-10 of the last 10 years of simulation, robust if it agrees on 7-8 years, and transitional if on 6 or fewer years.

887 **Table 1.** Simulations with different scenarios evaluated by INLAND model in Amazonia-Cerrado
888 transition. CA, climatological average, 1961-1990; CV, monthly climate data, 1948-2008; the nutrient
889 limitation on V_{max} - PC, no P limitation (V_{max} = 65 μmol-CO_2 m^{-2} s^{-1}); PR, regional P limitation; PG,
890 global P limitation).

			V_{max}		
Climate	**CO_2**	**Fire (F)**	**PC**	**PR**	**PG**
CA	Variable	Off	CA+PC	CA+PR	CA+PG
CA	Variable	On	CA+PC+F	CA+PR+F	CA+PG+F
CV	Variable	Off	CV+PC	CV+PR	CV+PG
CV	Variable	On	CV+PC+F	CV+PR+F	CV+PG+F

891

892

Table 2. Individual and combined effects for each simulation in Amazonia-Cerrado transition. CA, climatological seasonal average, 1961-1990; CV, monthly climate data, 1948-2008; the nutrient limitation on V_{max} - PC, no P limitation (V_{max} = 65 μmolCO_2 m^{-2} s^{-1}); PR, regional P limitation; PG, global P limitation)

Climate (C)	**Phosphorus (P)**	**Fire (F)**
(CV+PC)-(CA+PC)	(CA+PR)-(CA+PC)	(CA+PC+F)-(CA+PC)
(CV+PR)-(CA+PR)	(CV+PR)-(CV+PC)	(CV+PC+F)-(CV+PC)
(CV+PG)-(CA+PG)	(CA+PG)-(CA+PC)	(CA+PR+F)-(CA+PR)
	(CV+PG)-(CV+PC)	(CV+PR+F)-(CV+PR)
		(CA+PG+F)-(CA+PG)
		(CV+PG+F)-(CV+PG)

Table 3. Summary of average NPP, LAI and AGB for the Amazonia-Cerrado transition at the transects domains, considering all simulations with CA and CV regardless of fire presence or P limitation. The results of a one-way ANOVA are also shown, including the *F* statistic, and p value. Values within each column followed by a different letter are significantly different ($p < 0.05$) according to the Tukey–Kramer test (n=1860: 31 pixels x 10 years x $n_{simulation/2}$).

Group 1	**NPP**		**LAI_{total}**		**LAI_{lower}**		**LAI_{upper}**		**AGB**	
	kg-C m^{-2} yr^{-1}		m^2 m^{-2}		m^2 m^{-2}		m^2 m^{-2}		kg-C m^{-2}	
CA	0.68	a	7.47	a	1.98	a	5.49	a	6.68	a
CV	0.64	b	7.15	b	2.11	a	5.04	b	6.30	b
F	*40.2*		*57.2*		*2.96*		*36.0*		*11.3*	
p	*<0.001*		*<0.001*		*ns*		*<0.01*		*<0.001*	

Table 4. Summary of average NPP, LAI and AGB for the transition at the transects domains, considering different P limitation, regardless of climate and fire presence. The results of a one-way ANOVA are also shown, including the *F* statistic, and p value. Values within each column followed by a different letter are significantly different ($p < 0.05$) according to the Tukey–Kramer test (n=1240: 31 pixels x 10 years x $n_{simulation/3}$).

Group 2	**NPP**		**LAI_{total}**		**LAI_{lower}**		**LAI_{upper}**		**AGB**	
	kg-C m^{-2} yr^{-1}		m^2 m^{-2}		m^2 m^{-2}		m^2 m^{-2}		kg-C m^{-2}	
PC	0.71	a	7.64	a	1.84	b	5.80	a	7.15	a
PR	0.64	b	7.15	b	2.19	a	4.95	b	6.20	b
PG	0.64	b	7.14	b	2.10	a	5.04	b	6.12	b
$F_{2.99}$	*62.8*		*61.0*		*8.75*		*53.5*		*33.6*	
p	*<0.001*		*<0.001*		*<0.01*		*<0.01*		*<0.001*	

Table 5. Summary of average NPP, LAI and AGB for the transition at the transects domains, considering presence or absence of fire. The results of a one-way ANOVA are also shown, including the *F* statistic, and p value. Values within each column followed by a different letter are significantly different ($p < 0.05$) according to the Tukey–Kramer test (n=1860: 31 pixels x 10 years x $n_{simulation/2}$).

Group 3	**NPP**		**LAI_{total}**		**LAI_{lower}**		**LAI_{upper}**		**AGB**	
	kg-C m^{-2} yr^{-1}		m^2 m^{-2}		m^2 m^{-2}		m^2 m^{-2}		kg-C m^{-2}	
Fire OFF	0.66	a	6.72	b	0.88	b	5.84	a	8.47	b
Fire ON	0.67	b	7.90	a	3.21	a	4.69	b	4.51	a
$F_{3.84}$	*8.28*		*937*		1459		249		1719	
p	*<0.005*		*<0.001*		*<0.01*		*<0.01*		*<0.001*	

Table 6. Summary of average NPP, LAI and AGB for the transition at the transects domains, considering all factor combinations. The results of a one-way ANOVA are also shown, including the *F* statistic, and p value. Values within each column followed by a different letter are significantly different ($p < 0.05$) according to the Tukey–Kramer test (n=310: 31 pixels x 10 years).

	NPP		**LAI_{total}**		**LAI_{lower}**		**LAI_{upper}**		**AGB**	
	kg-C m^{-2} yr^{-1}		m^2 m^{-2}		m^2 m^{-2}		m^2 m^{-2}		kg-C m^{-2}	
CV+PC	0.69	bcd	6.96	d	0.84	e	6.48	a	9.01	ab
CV+PG	0.61	f	6.24	f	0.85	e	5.60	bc	7.91	c
CV+PR	0.62	f	6.33	f	0.85	e	5.74	bc	8.04	c
CV+PC+F	0.69	abc	7.92	b	2.91	cd	4.61	ef	4.89	de
CV+PG+F	0.63	ef	7.76	b	3.73	a	5.81	bc	3.91	f
CV+PR+F	0.63	ef	7.65	bc	3.47	ab	4.69	ef	4.02	f
CA+PC	0.72	ab	7.39	c	0.91	e	6.12	ab	9.31	a
CA+PG	0.64	def	6.64	e	0.91	e	5.40	cd	8.22	c
CA+PR	0.65	cdef	6.72	de	0.91	e	5.49	cd	8.31	bc
CA+PC+F	0.74	a	8.29	a	2.69	d	5.02	de	5.40	d
CA+PG+F	0.67	cde	7.90	b	3.29	abc	4.04	g	4.45	ef
CA+PR+F	0.67	cde	7.88	b	3.19	bc	4.18	fg	4.42	ef
F	*16.2*		*115*		*140*		38.1		*172*	
p	*<0.001*		*<0.001*		*<0.01*		*<0.01*		*<0.001*	

924 **Table 7**. Correlation coefficients of AGB simulated by INLAND and field estimates (n= 310: 31 pixels

925 x 10 years).

	T1	T2	T3	T4	T5	All transects
CA+PC	0.843	0.928	0.886	0.937	0.337	0.786
CV+PC	0.838	0.884	0.890	0.939	0.355	0.781
CA+PR	0.793	0.848	0.830	0.911	0.399	0.756
CV+PR	0.795	0.793	0.832	0.907	0.527	0.771
CA+PG	0.814	0.951	0.838	0.889	0.388	0.776
CV+PG	0.825	0.922	0.840	0.879	0.496	0.792
CA+PC+F	0.988	0.987	0.977	0.892	0.133	0.795
CV+PC+F	0.976	0.947	0.933	0.908	0.187	0.790
CA+PR+F	0.842	0.805	0.981	0.808	0.561	0.799
CV+PR+F	0.925	0.804	0.927	0.808	0.319	0.757
CA+PG+F	0.844	0.961	0.980	0.830	0.430	0.809
CV+PG+F	0.845	0.932	0.931	0.881	0.177	0.753
CA avg	0.854	0.913	0.915	0.878	0.375	0.787
CV avg	0.867	0.880	0.892	0.887	0.344	0.774

926